Genomes & Developmental Control

The unique and cooperative roles of the *Grainy head*-like transcription factors in epidermal development reflect unexpected target gene specificity

Yeliz Boglev [a], Tomasz Wilanowski [a,1], Jacinta Caddy [a], Vishwas Parekh [b], Alana Auden [a], Charbel Darido [a], Nikki R. Hislop [a], Michael Cangkrama [a], Stephen B. Ting [a,2], Stephen M. Jane [a,c,*]

[a] *Bone Marrow Research Laboratories, Melbourne Health Research Directorate, c/o Royal Melbourne Hospital Post Office, Parkville, Victoria 3050, Australia*
[b] *Department of Pediatrics, and The Committee on Developmental Biology, University of Chicago, Chicago, IL 60637, USA*
[c] *Department of Medicine, University of Melbourne, Parkville, Victoria 3050, Australia*

ARTICLE INFO

ABSTRACT

The *Grainy head*-like 3 (*Grhl3*) gene encodes a transcription factor that plays essential roles in epidermal morphogenesis during embryonic development, with deficient mice exhibiting failed skin barrier formation, defective wound repair, and loss of eyelid fusion. Despite sharing significant sequence homology, overlapping expression patterns, and an identical core consensus DNA binding site, the other members of the *Grhl* family (*Grhl1* and *-2*) fail to compensate for the loss of *Grhl3* in these processes. Here, we have employed diverse genetic models, coupled with biochemical studies, to define the inter-relationships of the *Grhl* factors in epidermal development. We show that *Grhl1* and *Grhl3* have evolved complete functional independence, as evidenced by a lack of genetic interactions in embryos carrying combinations of targeted alleles of these genes. In contrast, compound heterozygous *Grhl2*/*Grhl3* embryos displayed failed wound repair, and loss of a single *Grhl2* allele in *Grhl3*-null embryos results in fully penetrant eyes open at birth. Expression of *Grhl2* from the *Grhl3* locus in homozygous knock-in mice corrects the wound repair defect, but these embryos still display a complete failure of skin barrier formation. This functional dissociation is due to unexpected differences in target gene specificity, as both GRHL2 and GRHL3 bind to and regulate expression of the wound repair gene *Rho GEF 19*, but regulation of the barrier forming gene, *Transglutaminase 1* (*TGase1*), is unique to GRHL3. Our findings define the mechanisms underpinning the unique and cooperative roles of the *Grhl* genes in epidermal development.

Introduction

The mammalian skin lies at the interface between the internal organs and the environment, and plays a crucial role in the body's defence mechanisms. The outer most layer, the epidermis, is essential for establishment and maintenance of the barrier function of the skin, integrating the body's physiology with the terrestrial environment (Proksch et al., 2008; Segre, 2006). The epidermal barrier works in two directions, preventing excessive fluid loss from within, and impeding the entry of extraneous microorganisms and toxins. In the mouse, the epidermal barrier is established between embryonic day (E) 16.5 and 18.5 in a wave that is initiated dorsally and spreads to the ventral surface (Hardman et al., 1998). Defects in barrier formation have been described in a wide variety of mouse mutants emphasising the complexity of this process. These mutations involve genes encoding epidermal structural proteins, lipid biosynthesis and protein/lipid cross-linking enzymes, intercellular junction proteins, and transcription factors (Jane et al., 2005; Madison, 2003; Segre, 2003).

In addition to its barrier function, the epidermis and its embryonic tissue of origin, the non-neural ectoderm play pivotal roles in a range of developmental events requiring coordinated cellular movement. These epidermal morphogenetic events include embryonic wound repair (Jacinto et al., 2001; Martin, 1996), neural tube closure (Colas and Schoenwolf, 2001; Hackett et al., 1997), and in the mouse, fusion of the eyelids before birth (Findlater et al., 1993; Grose, 2003; Xia and Karin, 2004). The epidermally expressed genes known to be involved in these processes are diverse, and largely differ from those regulating the establishment of the skin barrier. One exception to this is the gene encoding the transcription factor *Grainy head-like 3* (*Grhl3*), which is expressed in the epidermis from E8.5 of development into adulthood (Auden et al., 2006; Ting et al., 2003b). Mice lacking this gene fail to form the epidermal barrier (Ting et al., 2005; Yu et al., 2006), and exhibit defective neural tube closure (Ting et al., 2003a), and

---

* Corresponding author. Bone Marrow Research Laboratories, c/o Royal Melbourne Hospital Post Office, Grattan Street, Parkville, Victoria 3050, Australia. Fax: +61 3 93428634.

E-mail address: jane@wehi.edu.au (S.M. Jane).
[1] Present address: Laboratory of Signal Transduction, Nencki Institute of Experimental Biology, 02-093 Warsaw, Poland.
[2] Present address: Cell Cycle and Cancer Genetics Laboratory, Peter MacCallum Cancer Centre, Melbourne, Victoria 3002, Australia.

embryonic wound repair (Caddy et al., 2010; Ting et al., 2005). They also exhibit failed eyelid fusion manifesting as eyes open at birth (EOB) (Hislop et al., 2008; Yu et al., 2008), the penetrance of which is influenced by genetic background, and the co-deletion of the GRHL3 partner protein LMO4 (Hislop et al., 2008). As a transcription factor, the developmental roles of *Grhl3* are mediated through regulation of critical target genes. In the setting of skin barrier formation, we have identified the *Transglutaminase 1* (*TGase 1*) gene as a key downstream effector (Ting et al., 2005). In epidermal wound repair, *Grhl3* has been shown to function in the planar cell polarity (PCP) signalling pathway through direct transcriptional regulation of the *RhoA* activator, *Rho GEF 19* (Caddy et al., 2010).

Grhl3 is one of three mammalian members of the highly conserved *Grainy head-like* (*Grhl*) gene family that regulates the formation and maintenance of the integument in diverse species across 700 million years of evolution (Kudryavtseva et al., 2003; Ting et al., 2003b; Venkatesan et al., 2003; Wilanowski et al., 2002). The ancestral member of the family, *Drosophila grainy head* (*grh*) is expressed predominantly in the surface ectoderm (Biggin and Tjian, 1988; Dynlacht et al., 1989; Uv et al., 1997), and perturbed expression during development leads to phenotypes reminiscent of the *Grhl3*-null mice, with defective cuticle formation (Ostrowski et al., 2002), PCP-mediated defects in wing hair orientation (Lee and Adler, 2004), abnormal wound repair (Mace et al., 2005), and dorsal hole (Attardi et al., 1993), a paradigm for other epithelial closures, including wound healing in vertebrates (Jacinto and Martin, 2001). Flies lacking *grh* also display abnormalities of the head skeleton (Bray and Kafatos, 1991), and defective cellular adhesion (Narasimha et al., 2008). These phenotypes are mirrored by the *Grhl2* and *Grhl1* knockout mice, which exhibit failed craniofacial fusion and cranioschisis (Rifat et al., 2010), and perturbed epidermal desmosome formation, respectively (Wilanowski et al., 2008).

One paradox in the functions of the mammalian *Grhl* genes is their lack of redundancy, despite overlapping expression patterns in the surface ectoderm during development (Auden et al., 2006). *Grhl3* and *Grhl2* are co-expressed from E8.5 until E14.5, when the levels of expression of *Grhl2* are reduced and maintained at a lower level until birth. In contrast, *Grhl1* is not expressed in the surface ectoderm until E12.5, but its expression pattern is identical to that of *Grhl3* thereafter. Despite this, neither *Grhl1* nor *Grhl2* compensates for the loss of *Grhl3* in epidermal development. This paradox is further emphasized by the substantial sequence homology between the factors in the DNA-binding and protein dimerisation domains (Ting et al., 2003b; Wilanowski et al., 2002), and by our demonstration that the core consensus DNA binding sites of both GRHL1 and GRHL2 are identical to the site defined for GRHL3 (Ting et al., 2005; Wilanowski et al., 2008; Rifat et al., 2010).

In the current study, we explore the interactions between the mammalian *Grhl* members in the context of epidermal development utilizing compound knockout mouse lines, and a knock-in line, in which *Grhl2* is expressed from the *Grhl3* regulatory elements. Our findings provide important insight into the molecular mechanisms underlying skin barrier formation and epidermal morphogenesis.

Materials and methods

Mice

The generation and genotyping of *Grhl1*$^{+/-}$ (Wilanowski et al., 2008), *Grhl2*$^{+/-}$ and *Grhl3*^{2ki} (Rifat et al., 2010), and *Grhl3*$^{+/-}$ (Ting et al., 2003a) mice have been described previously. All mouse lines were generated and maintained on a C57Bl/6 background. Mice were housed under standard conditions in a 12-h dark/light cycle with food and water ad libitum. For embryo collection, adult female mice were mated overnight and the gestational age was determined from the vaginal plug, the appearance of which was designated as gestational

day 0.5. Animal experiments were pre-approved by The University of Melbourne Animal Ethics Committee.

Histology and immunohistochemistry (IHC)

For histological analysis, samples were collected at E8.5 to E18.5, fixed in 4% paraformaldehyde (4% PFA) overnight at 4 °C, embedded in paraffin and stained with hematoxylin and eosin (H&E). For IHC, embryos at the time points of interest were collected and fixed in 4% PFA overnight, embedded in paraffin and sectioned at 8 μm onto Superfrost-Plus slides and processed as per standard protocols using DAB staining. Primary polyclonal antibodies were purchased from Covance (CA, USA) and were used at the following dilutions: K5, K6 and K10 (1:1000), involucrin (1:500) and filaggrin (1:1000). F-actin staining of whole-mount eyelids was carried out using eye samples from embryos fixed in 4% PFA in PBS at 4 °C overnight. The anterior portion of the eye, together with surrounding epidermal tissue and intact eyelids, was dissected from fixed tissue and incubated with Rhodamine-phalloidin at 1:1000 and counter-stained with DAPI (1:1000) to visualise nuclei. Samples were then observed with a fluorescence microscope according to standard protocols.

In situ hybridisation

For in situ hybridisation, embryos were fixed in 4% PFA at 4 °C overnight, embedded in paraffin and 7 μm sections collected onto gelatin-coated slides. In situ hybridisation was then undertaken as described previously (Auden et al., 2006), utilising a probe specific for the *Grhl3*^{2ki} transcript (rabbit β-globin polyA tail, nucleotides 12172–13366 in Bluescript II SK plasmid) or *Grhl2* (Wilanowski et al., 2002).

Skin permeability and embryonic wound healing assays

Skin permeability assays were undertaken at E17.5, and analysis of wound repair was performed at E12.5 as described previously (Ting et al., 2005). At least 6 embryos of each genotype were analysed for each of the assays. Failed wound repair was defined as a residual defect >80% of the original wound diameter. A Fisher's exact test was used to determine statistical difference between wound healing for the different genotypes. *P* values ≤0.05 were considered significant, and results were analysed using the computer software program Prism (GraphPad).

Scanning electron microscopy (SEM)

For SEM, E12.5 wound culture embryos, or E15.5–17.5 day eyelids were fixed overnight in 2.5% glutaraldehyde and post-fixed in 1% osmium tetroxide (OsO_4). After fixation, samples were dehydrated through graded acetone solutions (70–100%), critical point dried (Polaron critical point dryer, Quroum Technologies, East Sussex, UK), mounted on stubs and observed using a Philips 515 SEM at 20kv (Philips, Amsterdam, Netherlands). At least 6 embryos of each genotype were observed at each time point.

Electrophoretic mobility shift assay (EMSA), chromatin immunoprecipitation (ChIP) and position weight matrix (PWM) determination

EMSAs were performed using rGRHL2 and rGRHL3 as previously described (Wilanowski et al., 2008). The following oligonucleotide probes were utilized (sense strand only given):

Grhl consensus: 5′-AACTATAAAACCGGTTTATCTAGTTGG-3′
TGase1: 5′-TGTTCCTGGAGCCGGTTGGTCTGGAT-3′
Rho GEF 19: 5′CCTGACTGGCCAAACCGGTTCTGGGGAAGGGG-3′

The ChIP experiment followed the published protocol (Forsberg et al., 2000).

Primers specific for the human *Rho GEF 19* promoter were:
5′-TCTTTCGGACCTGGGTCTAG-3′
5′-AAGCTCCTGGGTATTGTGTG-3′
The PWM was determined using the JASPAR algorithm (Vlieghe et al., 2006).

Q-RT-PCR

To quantitate gene expression in wild-type, $Grhl3^{+/2ki}$, and $Grhl3^{2ki/2ki}$ E18.5 embryos, dorsal skin was dissected and the epidermis separated from the dermis following enzyme treatment with 2 mg/ml Dispase II (Invitrogen, San Diego, CA, USA) at 4 °C overnight. Separated epidermal and dermal samples were homogenised in TRIzol (Invitrogen) and RNA was extracted in accordance to the manufacturer's recommendations. Q-PCR was carried out as described previously (Ting et al., 2003a) using the following primers.
Mouse *Rho GEF 19* sense 5′-GAAGTCAGCCTGGAAACTGC-3′
Mouse *Rho GEF 19* antisense 5′-GATCCTGAGTCGGCTGTGCT-3′
Mouse *TGase1* sense 5'-GCCCTTGAGCTCCTCATTG-3'
Mouse *TGase1* antisense 5'-CCCTTACCCACTGGGATGAT-3'

Results

### Grhl3 and Grhl1 display no genetic interaction

To evaluate genetic interactions between *Grhl3* and the other mammalian *Grhl* genes, and to determine the effects of *Grhl* gene dosage on skin barrier formation and other epidermal morphogenetic events, we inter-crossed lines carrying the various *Grhl* targeted alleles. Our initial experiments focused on *Grhl1*, which displays a similar expression pattern to *Grhl3* in later embryogenesis (Auden et al., 2006). *Grhl1*-null mice are healthy and fertile, but display an initial delay in coat growth, with older mice exhibiting hair loss as a result of poor anchoring of the hair shaft in the follicle. These mice also develop palmoplantar keratoderma (PPK) due to loss of expression of *Desmoglein 1* (*Dsg1*), a critical direct target gene of GRHL1 (Wilanowski et al., 2008). Compound heterozygous mice ($Grhl1^{+/-}/Grhl3^{+/-}$) exhibited no defects in barrier formation, eyelid fusion or embryonic wound repair, and also displayed normal coat growth and palmoplantar skin (data not shown). Deletion of additional alleles of either gene failed to uncover any epistatic interactions, with skin barrier formation (not shown), eyelid fusion (Fig. 1A and Supplementary Table 1), and embryonic wound repair (Fig. 1B) in $Grhl1^{+/-}/Grhl3^{-/-}$ and $Grhl1^{-/-}/Grhl3^{-/-}$ embryos displaying phenotypes that reflected the genotype of *Grhl3* alone, and delayed coat growth (Fig. 1C) and increased palmoplantar skin thickness in $Grhl1^{-/-}/Grhl3^{+/-}$ mice (not shown) exactly mirroring the $Grhl1^{-/-}/Grhl3^{+/+}$ animals (Wilanowski et al., 2008). The latter two phenotypes could not be assessed in $Grhl1^{-/-}/Grhl3^{-/-}$ mice due to their early lethality, but expression of *Dsg1* is not altered in the skin of E18.5 $Grhl3^{-/-}$ or $Grhl1^{-/-}/Grhl3^{-/-}$ embryos (Yu et al., 2006, and data not shown). Consistent with these findings, we demonstrated by ChIP analysis that GRHL3 was unable to bind to the region of the *Dsg1* promoter targeted by GRHL1, and that GRHL1 did not bind to the critical GRHL3-responsive elements in either the *TGase1* or *Rho GEF 19* genes (Fig. 1D). This latter result was surprising, given that the core DNA consensus binding site for GRHL1 and GRHL3 defined by CASTing assays is identical (Ting et al., 2005; Wilanowski et al., 2008). To address this, we assembled a position weight matrix (PWM) for each of the factors, based on our CASTing data (Fig. 1E). Although, as reported previously, the core DNA consensus binding site of the two factors was identical, substantial differences in the PWMs were evident at both flanking nucleotides, and within the consensus itself, suggesting the potential for differences in binding site specificity. When taken in context with our ChIP data, our findings indicate that *Grhl3* and *Grhl1* have evolved completely disparate functions in the context of epidermal development due predominantly to diverse target gene selectivity.

A genetic interaction between Grhl2 and Grhl3 in embryonic wound repair

Our next experiments focused on *Grhl2*, as the early epidermal expression patterns of *Grhl2* and *Grhl3* overlap (Auden et al., 2006), and the embryonic lethality of *Grhl2*-null mice (at embryonic day (E) 11.5) with severe neural tube defects precludes analysis of skin barrier formation, embryonic wound repair, and eyelid fusion (Rifat et al., 2010). Timed pregnancies from matings of mice heterozygous for a targeted allele at either locus were examined at E18.5 (skin barrier and EOB), and at E12.5 (embryonic wound repair). Skin histology at E18.5 appeared normal in the compound heterozygous mice ($Grhl2^{+/-}/Grhl3^{+/-}$) when compared with wild-type or single heterozygous littermate controls (Fig. 2A, upper panel, and data not shown). Consistent with this, no defect in skin barrier formation was observed in any embryo (Fig. 2A, lower panel). Eyelid fusion also proceeded normally in these animals (Fig. 2A, lower panel). However, defective embryonic wound repair was seen with the $Grhl2^{+/-}/Grhl3^{+/-}$ mice that was never observed in the single heterozygotes (Fig. 2B). These findings indicate that *Grhl2* and *Grhl3* function cooperatively in embryonic wound repair, but not in formation of the barrier.

Grhl2 and Grhl3 exhibit functional redundancy in eyelid fusion

To determine whether functional redundancies between the *Grhl* factors could be uncovered with loss of additional alleles, we initially generated mice lacking the *Grhl3* gene, and heterozygous for the targeted *Grhl2* allele. $Grhl3^{-/-}$ embryos fail to establish an epidermal barrier, and display defective embryonic wound repair (Ting et al., 2005), but on the C57Bl/6 background of the knockout line, eyelid fusion is indistinguishable from wild-type litter mates, exhibiting no delay in closure (Fig. 3A and B) (Hislop et al., 2008). As expected, barrier formation and wound repair were markedly defective in the $Grhl2^{+/-}/Grhl3^{-/-}$ embryos (data not shown). In addition, EOB was observed in all embryos, despite both lines being generated on the C57Bl/6 background (Fig. 3C and Supplementary Table 1). Eyelid formation during mouse embryogenesis initiates at E11.5, when the ectodermal grooves form on either side of the eye. At E13.5 mesenchymal protrusions begin to form the new eyelid roots that extend towards the centre of the eye. Between E14.5 and E16.5, a ridge of epithelial cells begins to form at the apex of the nascent upper and lower eyelids, and subsequently extends across the surface of the eye, while the mesenchymal root tracks behind. Fusion only occurs between the epithelium of the upper and lower eyelid, while the mesenchymal tissue remains separate in preparation for re-opening of the eyelids approximately 2 weeks after birth (Findlater et al., 1993). The defect in eyelid closure in mice lacking *Grhl3* (on different backgrounds) is due to failed migration of the leading edge surface ectodermal cells (Hislop et al., 2008). At E15.5 we observed groove formation and the appearance of mesenchymal protrusions, but no evidence of epithelial migration in the $Grhl2^{+/-}/Grhl3^{-/-}$ embryos compared with either $Grhl3^{-/-}$ or wild-type controls (Fig. 3D–F). Consistent with this, expression of *Grhl2* was maximal in the leading edge cells, analogous to *Grhl3* (Fig. 3G and H). SEM at E15.5 demonstrated clusters of epidermal cells appearing at the margins of the eyelid root in the wild-type mice that were not observed in the $Grhl2^{+/-}/Grhl3^{-/-}$ embryos (Fig. 3I–N). A hallmark of eyelid closure is the formation of an actin cable at the leading edge of epidermal migration, coupled with actin polymerisation and stress fiber formation more laterally (Xia and Karin, 2004; Zhang et al., 2003). Using whole-mount rhodamine-phalloidin staining as a marker of actin polymerisation, we examined actin cable formation in the control and mutant embryos. At E15.5, wild-type embryos displayed pronounced actin cable formation at the leading and radial margins, in stark contrast to the weak phalloidin staining observed in $Grhl2^{+/-}/Grhl3^{-/-}$ eyelids (Fig. 3O and P). Coupled with our earlier data, these
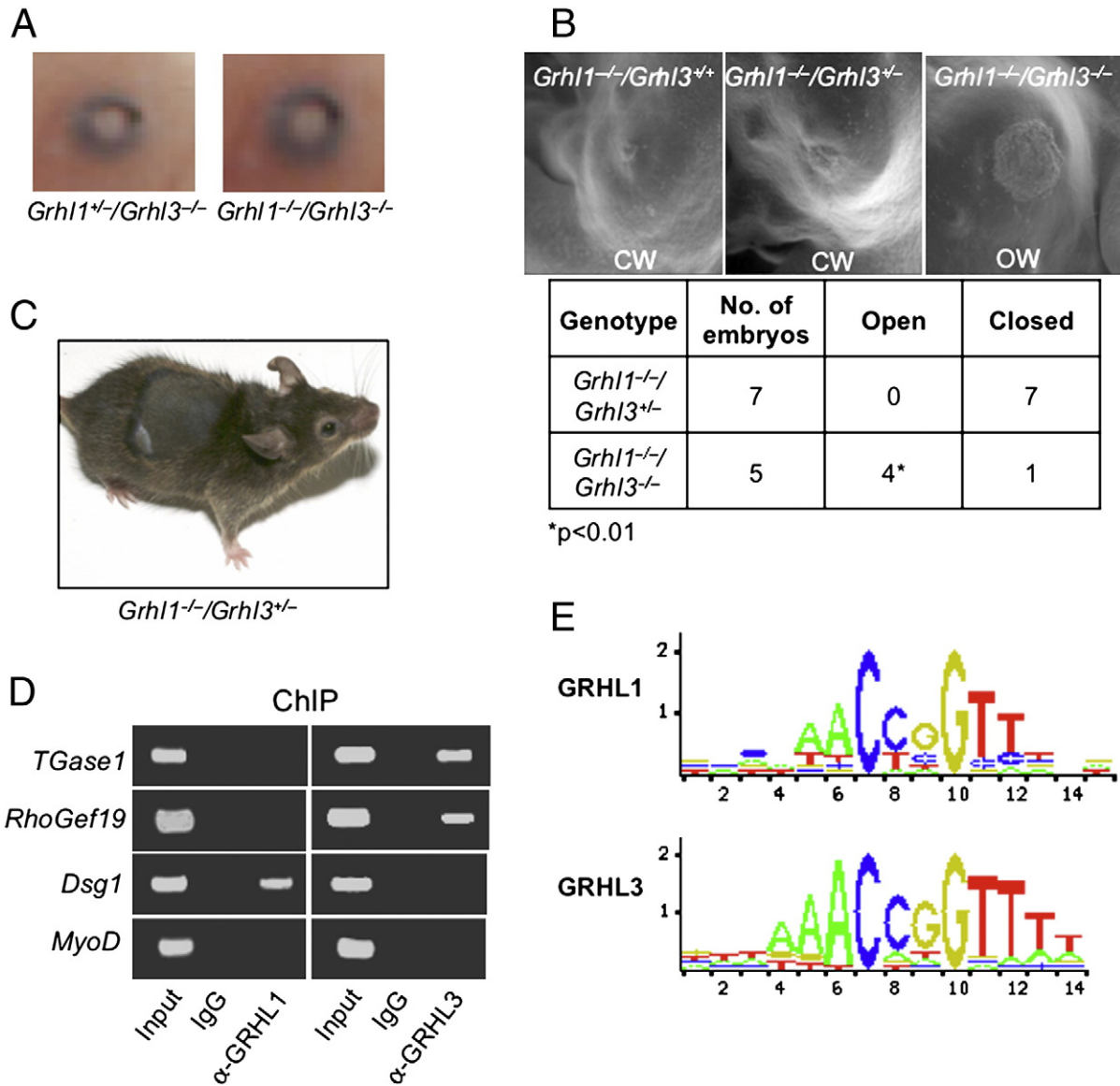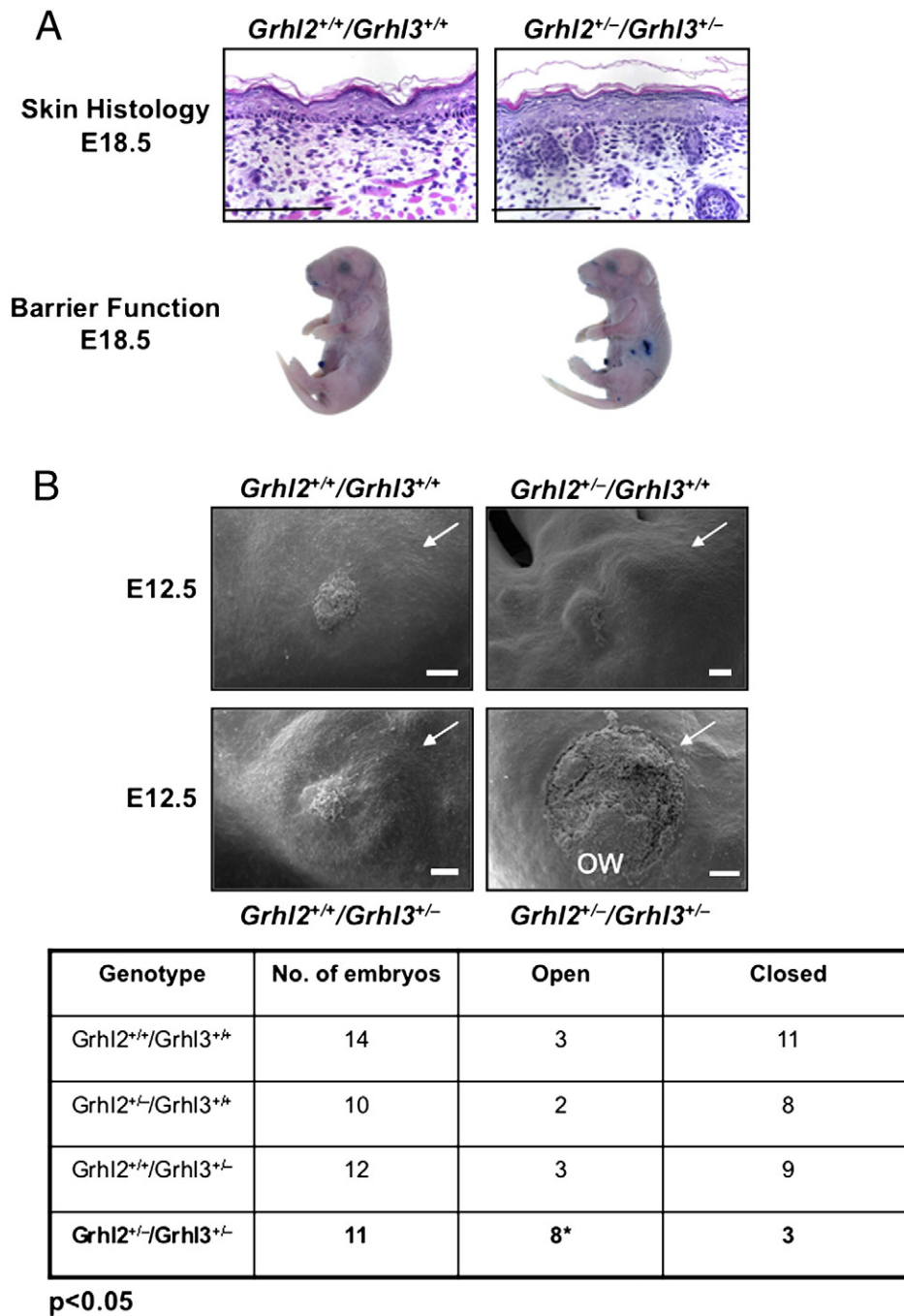
Fig. 1. *Grhl1* and *Grhl3* display no functional cooperativity due to diverse target gene selectivity. (A) Normally fused eyelids in *Grhl1* $^{+/-}$/*Grhl3* $^{-/-}$ and *Grhl1* $^{-/-}$/*Grhl3* $^{-/-}$ embryos at E18.5. (B) SEM of a hind limb amputation wound after 24 h in culture in *Grhl1* $^{-/-}$/*Grhl3* $^{+/+}$, *Grhl1* $^{-/-}$/*Grhl3* $^{+/-}$, and *Grhl1* $^{-/-}$/*Grhl3* $^{-/-}$ embryos at E12.5. All images are representative of at least 5 embryos of each genotype. ow, open wound. Scale = 100 μm. The table is a summary of the wound healing data for the respective genotypes. A Fisher's exact test was used to determine statistical difference between wound healing for the different genotypes. *P* values ≤0.05 were considered significant. (C) Regional hair loss in a *Grhl1* $^{-/-}$/*Grhl3* $^{+/-}$ mouse that mirrors the loss in *Grhl1* $^{-/-}$ mice (Wilanowski et al., 2008). (D) ChIP analysis of GRHL1 and GRHL3 binding to *Tgase1*, *Rho GEF 19*, *Dsg1*, and the negative control *MyoD* regulatory elements. Chromatin from HaCAT cells was immunoprecipitated using antisera to either GRHL1 or GRHL3. Pre-immune sera (IgG) served as a negative control. The input chromatin is shown. The immunoprecipitated chromatin was amplified with the stated primers. (E) PWM of GRHL1 and GRHL3 DNA binding sites.

findings indicate that *Grhl2* and *Grhl3* exhibit functional redundancy in epidermal morphogenetic events.

Grhl2 is unable to replace Grhl3 in establishment of the epidermal barrier

The non-redundant functions of *Grhl2* and *Grhl3* in skin barrier formation were observed despite the two genes exhibiting substantial sequence homology, displaying overlapping expression patterns in the surface ectoderm throughout much of embryogenesis, and demonstrating functional cooperativity in both eyelid fusion and embryonic wound repair. This dichotomy was emphasized further by our demonstration that the core consensus DNA binding site for GRHL2 was identical to the site previously defined for GRHL3 (Ting et al., 2005; Rifat et al., 2010). Comparative analysis of the PWMs of GRHL2 and GRHL3 revealed similarities in both the core and flanking

nucleotides that were not shared with GRHL1 (Fig. 4A). Nevertheless, differences in the GRHL2 and GRHL3 matrices were still observed, raising the possibility that differential target gene selectivity could still underpin the functional differences between these factors. To address this, we designed a knock-in model, in which *Grhl2* expression was regulated by the *Grhl3* genomic locus, as a stringent genetic test to further explore the functional equivalence of the two genes (Rifat et al., 2010). Using primers specific for the *Grhl3* and knock-in (*Grhl3* ^{2ki}) transcripts we demonstrated that the knock-in allele was expressed in the epidermis of both the +/2ki and 2ki/2ki animals, but not in the wild-type controls (Fig. 4B). In contrast, endogenous *Grhl3* expression was seen in the wild-type and ki/+ heterozygous mice, but not in the 2ki/2ki homozygous mice (Fig. 4B). This was confirmed by in situ hybridisation studies with *Grhl3* and *Grhl3* ^{2ki}-specific probes on E16.5 epidermis, immediately prior to the onset of barrier formation (Rifat et al., 2010). Endogenous *Grhl2* is

A

Skin Histology E18.5

Grhl2+/+/Grhl3+/+   *Grhl2+/−/Grhl3+/−*

Barrier Function E18.5

B

Grhl2+/+/Grhl3+/+   *Grhl2+/−/Grhl3+/+*

E12.5

E12.5

OW

Grhl2+/+/Grhl3+/−   *Grhl2+/−/Grhl3+/−*

Genotype	No. of embryos	Open	Closed
Grhl2+/+/Grhl3+/+	14	3	11
Grhl2+/−/Grhl3+/+	10	2	8
Grhl2+/+/Grhl3+/−	12	3	9
Grhl2+/−/Grhl3+/−	11	8*	3

p<0.05

Fig. 2. *Grhl3* and *Grhl2* function cooperatively in embryonic wound repair, but not skin barrier formation. (A) Skin histology from E18.5 embryos (upper panels), and skin barrier function in E17.5 embryos (lower panel) in wild-type and *Grhl2$^{+/−}$/Grhl3$^{+/−}$* mice. (B) SEM of a hind limb amputation wound after 24 h in culture in wild-type, *Grhl2$^{+/−}$/Grhl3$^{+/+}$*, *Grhl2$^{+/+}$/Grhl3$^{+/−}$*, and *Grhl2$^{+/−}$/Grhl3$^{+/−}$* embryos at E12.5. All images are representative of at least 10 embryos of each genotype. Arrows point to the boundary of the wound. ow, open wound. Scale = 100 μm. The table is a summary of the wound healing data for the respective genotypes. A Fisher's exact test was used to determine statistical difference between wound healing for the different genotypes. *P* values ≤0.05 were considered significant.

expressed at very low levels in the epidermis at this time (Auden et al., 2006). No alternate *Grhl3* transcripts were detectable in the *2ki/2ki* embryos using primers in exons distal to the knock-in cassette (data not shown).

We initially examined skin histology and barrier formation in *Grhl3$^{+/2ki}$* and wild-type control embryos. Consistent with the residual functional *Grhl3* allele in the *Grhl3$^{+/2ki}$* mice, no differences were observed between these two genotypes (data not shown). To examine the effects of *Grhl2* expression on epidermal barrier formation in the absence of *Grhl3*, *Grhl3$^{+/2ki}$* mice were inter-crossed

to yield homozygous knock-in embryos (*Grhl3$^{2ki/2ki}$*), or bred with *Grhl3$^{+/−}$* mice to generate *Grhl3$^{−/2ki}$* embryos. *Grhl3* mRNA expression was undetectable by PCR in embryos with both these genotypes (Fig. 4B and data not shown). As shown in Fig. 4C, both *Grhl3$^{2ki/2ki}$* and *Grhl3$^{−/2ki}$* embryos exhibited histological abnormalities in the epidermis that were identical to those observed in the *Grhl3*-null mice (Ting et al., 2005). These were accompanied by profound defects in barrier formation compared with a wild-type control (Fig. 4D). Our previous studies had identified the cross-linking enzyme, *TGase1* as a critical direct target gene of GRHL3 in the context of epidermal barrier
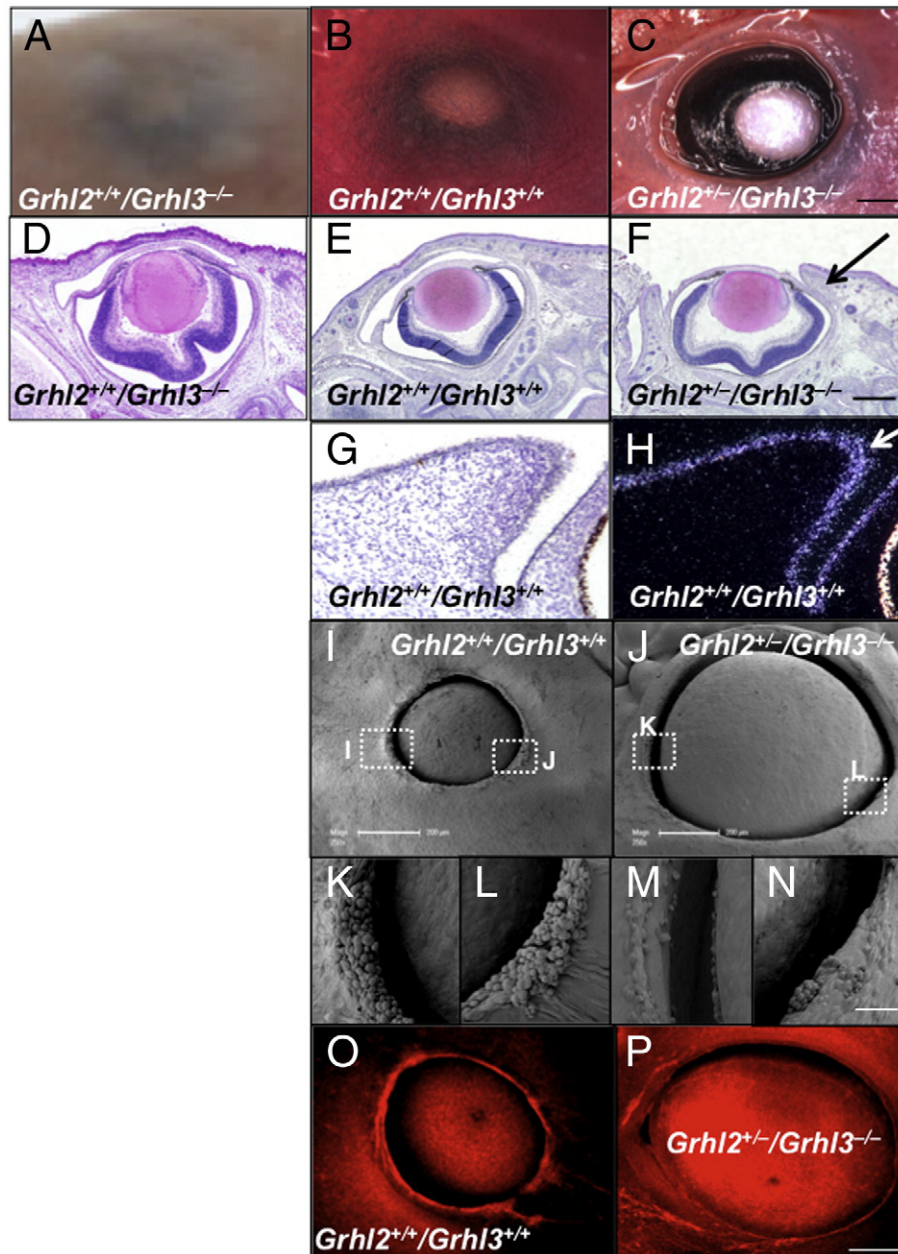
Fig. 3. *Grhl3* and *Grhl2* function cooperatively in embryonic eyelid fusion. (A–C) EOB in an E18.5 *Grhl2*$^{+/-}$/*Grhl3*$^{-/-}$ embryo, but not in the wild-type (*Grhl2*$^{+/+}$/*Grhl3*$^{+/+}$) or *Grhl2*$^{+/+}$/*Grhl3*$^{-/-}$ controls. (D–F) H&E staining of the coronal eye sections from wild-type, *Grhl2*$^{+/+}$/*Grhl3*$^{-/-}$ and *Grhl2*$^{+/-}$/*Grhl3*$^{-/-}$ embryos. The normal mesenchymal protrusion in the *Grhl2*$^{+/-}$/*Grhl3*$^{-/-}$ embryo is arrowed. Scale bar = 20 μm. (G and H) In situ hybridisation of the developing eyelid in a wild-type E15.0 embryo in bright-field (G) and dark field (H) with a *Grhl2*-specific probe demonstrating expression at the leading edge (arrowed). (I–N) SEM of developing eyelids of wild-type and *Grhl2*$^{+/-}$/*Grhl3*$^{-/-}$ E15.0 embryos. Clumps of cells are migrating inwards at the eyelid margin in the wild-type embryo (K and L), but are absent in the *Grhl2*$^{+/-}$/*Grhl3*$^{-/-}$ eyelid (M and N). Scale bar in I and J = 200uM. (O and P) Whole-mount staining of wild-type and *Grhl2*$^{+/-}$/*Grhl3*$^{-/-}$ eyelids at E15.0 was carried out using rhodamine-phalloidin to visualise F-actin. Actin fiber formation and radial F-actin cable are most prominent in the wild-type eyelids.

formation (Ting et al., 2005). GRHL3 binds to a region of the *TGase1* promoter that is essential for its tissue-specific expression in epidermis, and other epithelium. We examined this binding site in EMSAs with rGRHL3 and rGRHL2. As shown in Fig. 4E, a single protein/DNA complex was observed with the *TGase1* probe with rGRHL3 (lane 3). This complex was specifically competed with both an un-labelled *TGase1* probe (lane 4), and a probe containing the previously defined *Grhl* consensus sequence (lane 5), which is identical for all the members of the *Grhl* family. In contrast, rGRHL2 failed to bind to the *TGase1* probe (lane 2), but bound robustly to *Grhl* consensus probe (lane 6). This binding was specific as it was competed by excess unlabelled *Grhl* consensus probe (lane 7). Consistent with these findings, we

demonstrated that expression of *TGase1* was reduced in *Grhl3*$^{2ki/2ki}$ embryonic epidermis to a level comparable to that observed in *Grhl3*$^{-/-}$ embryos (Fig. 4F). Q-RT-PCR with epidermal and dermal-specific genes confirmed the integrity of the samples (Supplementary Fig. 1).

Altered expression of epidermal genes that are not direct targets of GRHL3, including keratin (K) 5, K6, K10, involucrin and filaggrin, has also been linked to the barrier defects in the *Grhl3*-null mice (Yu et al., 2006). We examined the expression of these genes using IHC in wild-type and *Grhl3*$^{2ki/2ki}$ E18.5 embryos (Fig. 5). The level and distribution of expression of all these genes in the *Grhl3*$^{2ki/2ki}$ mice differed from the wild-type embryos, and mirrored the defects observed in the *Grhl3*-null mice (Yu et al., 2006). Specifically, filaggrin, K5, and
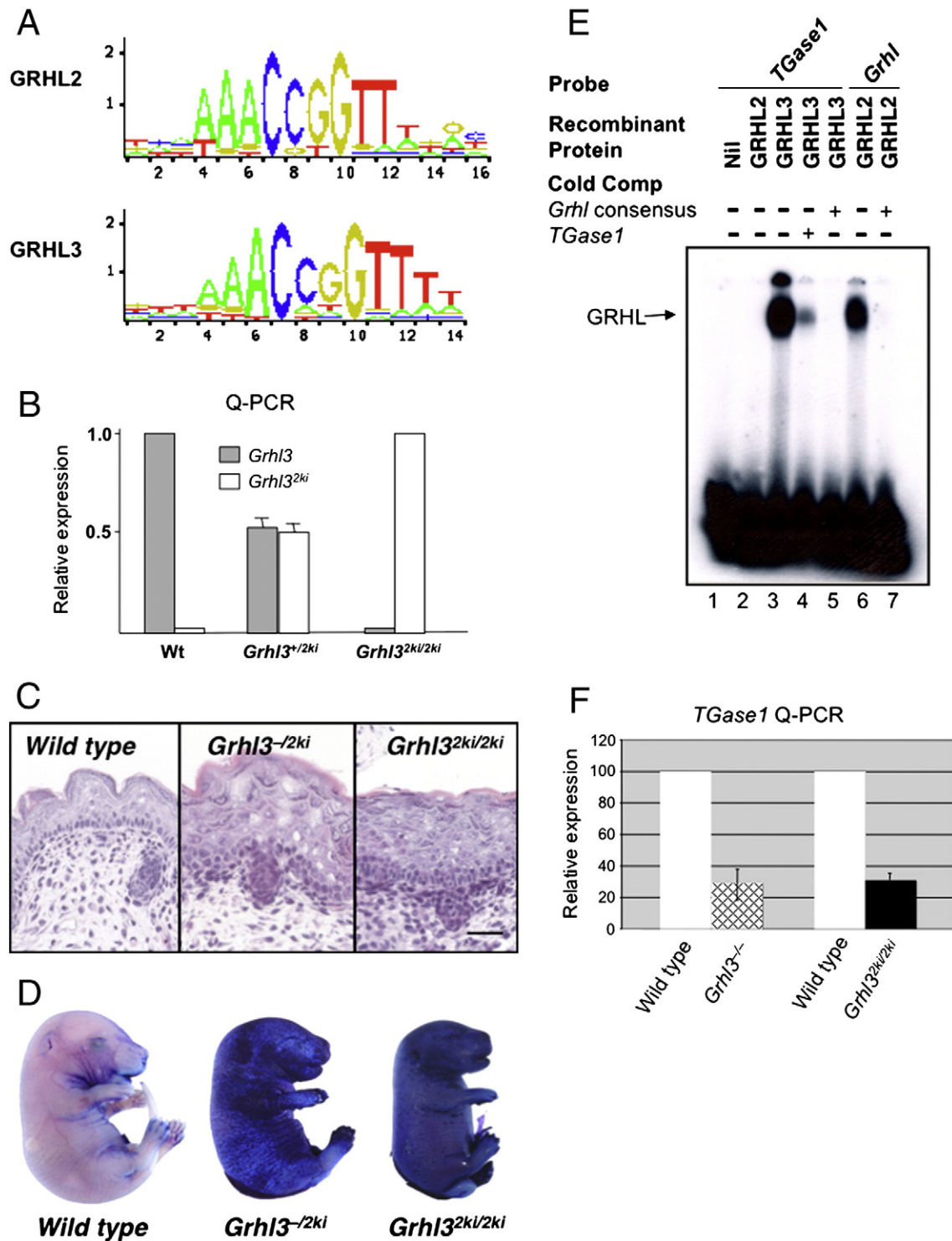
Fig. 4. *Grhl2* is unable to compensate for loss of *Grhl3* in skin barrier formation. (A) PWM of GRHL2 and GRHL3 DNA binding sites. (B) Q-RT-PCR analysis of the *Grhl3²ᵏⁱ* and *Grhl3* mRNA expression in E18.5 embryo epidermis from wild-type (Wt), *Grhl3⁺/²ᵏⁱ*, and *Grhl3²ᵏⁱ/²ᵏⁱ* mice. No expression of the *2ki* allele is seen in the wild-type embryos, and *Grhl3* is not expressed in the homozygous *Grhl3²ᵏⁱ/²ᵏⁱ* mice. (C) Skin histology from E18.5 wild-type, *Grhl3⁻/²ᵏⁱ*, and *Grhl3²ᵏⁱ/²ᵏⁱ* embryos. (D) Skin barrier function as measured by toluidine blue dye exclusion in E17.5 wild-type, *Grhl3⁻/²ᵏⁱ*, and *Grhl3²ᵏⁱ/²ᵏⁱ* embryos. (E) EMSA of rGRHL2 and rGRHL3 with *TGase1* and *Grhl* consensus probes. A 100-fold molar excess of unlabelled cold competitor probe was added in the indicated lanes. The migration of the GRHL/DNA complexes is arrowed. (F) Q-PCR of *TGase1* expression in wild-type (open columns), *Grhl3⁻/⁻* (hatched columns) and *Grhl3²ᵏⁱ/²ᵏⁱ* (closed columns) E18.5 epidermis. Bars represent standard errors. *HPRT* levels served as a reference.

particularly K6 showed expansion into layers where expression is not usually detected, whereas involucrin and to a lesser extent K10 exhibited reduced intensity. Taken together, these findings indicated that *Grhl2* was incapable of compensating for the loss of *Grhl3* in barrier formation and epidermal differentiation, even when expressed in the identical spatio-temporal profile.

Grhl2 compensates for loss of Grhl3 in embryonic wound repair

Our studies in the compound heterozygous mice indicated that *Grhl2* and *Grhl3* functioned cooperatively in embryonic wound repair. To determine whether their roles were identical in this process, we analysed the response to wounding in *Grhl3²ᵏⁱ/²ᵏⁱ* and *Grhl3⁻/²ᵏⁱ*
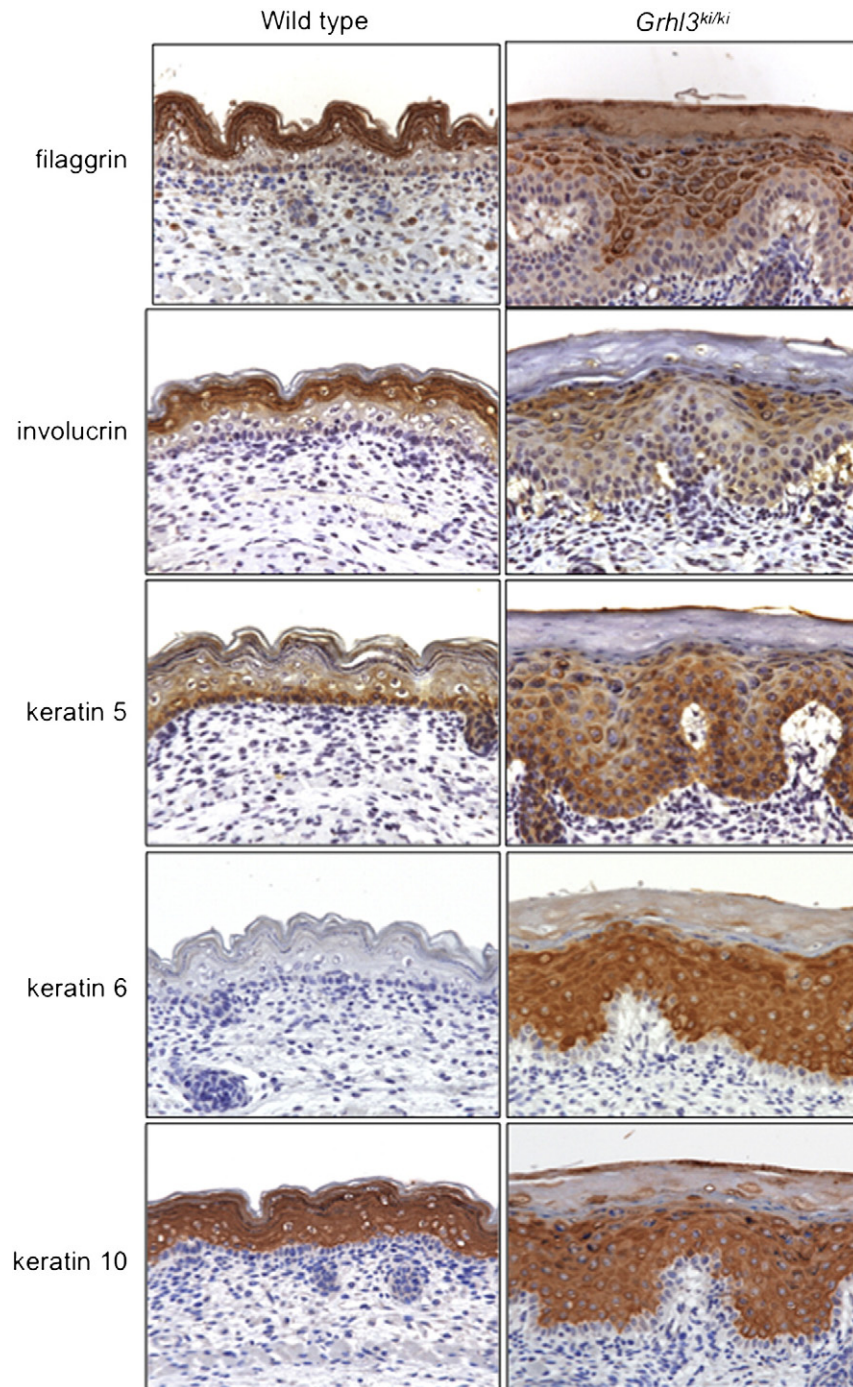
Fig. 5. Altered epidermal differentiation in $Grhl3^{2ki/2ki}$ embryos. IHC analysis of expression of filaggrin, involucrin, K5, K6, and K10 in epidermis from E18.5 wild-type and $Grhl3^{2ki/2ki}$ embryos.

embryos, and their wild-type controls (Fig. 6A). Healing of an amputated hind limb proceeded normally in animals of both genotypes, indicating that *Grhl2* and *Grhl3* are functionally synonymous in embryonic wound repair, which is only dependent on *Grhl* gene dosage, but not *Grhl* gene specificity. To decipher the mechanism underpinning this finding, we examined the ability of GRHL2 to bind to, and regulate the *Rho GEF 19* gene, the key GRHL3 target in the context of wound repair (Caddy et al., 2010). EMSA with a *Rho GEF 19* probe revealed binding of rGRHL2, which was specifically competed off in the presence of excess unlabeled *Grhl* consensus probe, or the *Rho GEF 19* probe (Fig. 6B). ChIP analysis confirmed specific binding of GRHL2 to the *Rho GEF 19* promoter (Fig. 6C), and consistent with this, expression of *Rho GEF 19* was increased 6-fold in the *Grhl3²ki/²ki*

epidermis compared to $Grhl3^{-/-}$ embryos (Fig. 6D). *Rho GEF 19* expression in the dermis, (where *Grhl3* is not expressed) was not altered. Although the expression level in the $Grhl3^{2ki/2ki}$ epidermis remains below that of wild-type embryos (Fig. 6D), functionally it exceeds the threshold required for successful embryonic epidermal wound repair.

Discussion

These studies explore the functional interactions between the mammalian *Grhl* genes in epidermal morphogenesis and development. We demonstrate that the *Grhl2* and *Grhl3* genes play overlapping roles in eyelid fusion and embryonic wound repair, with *Grhl*
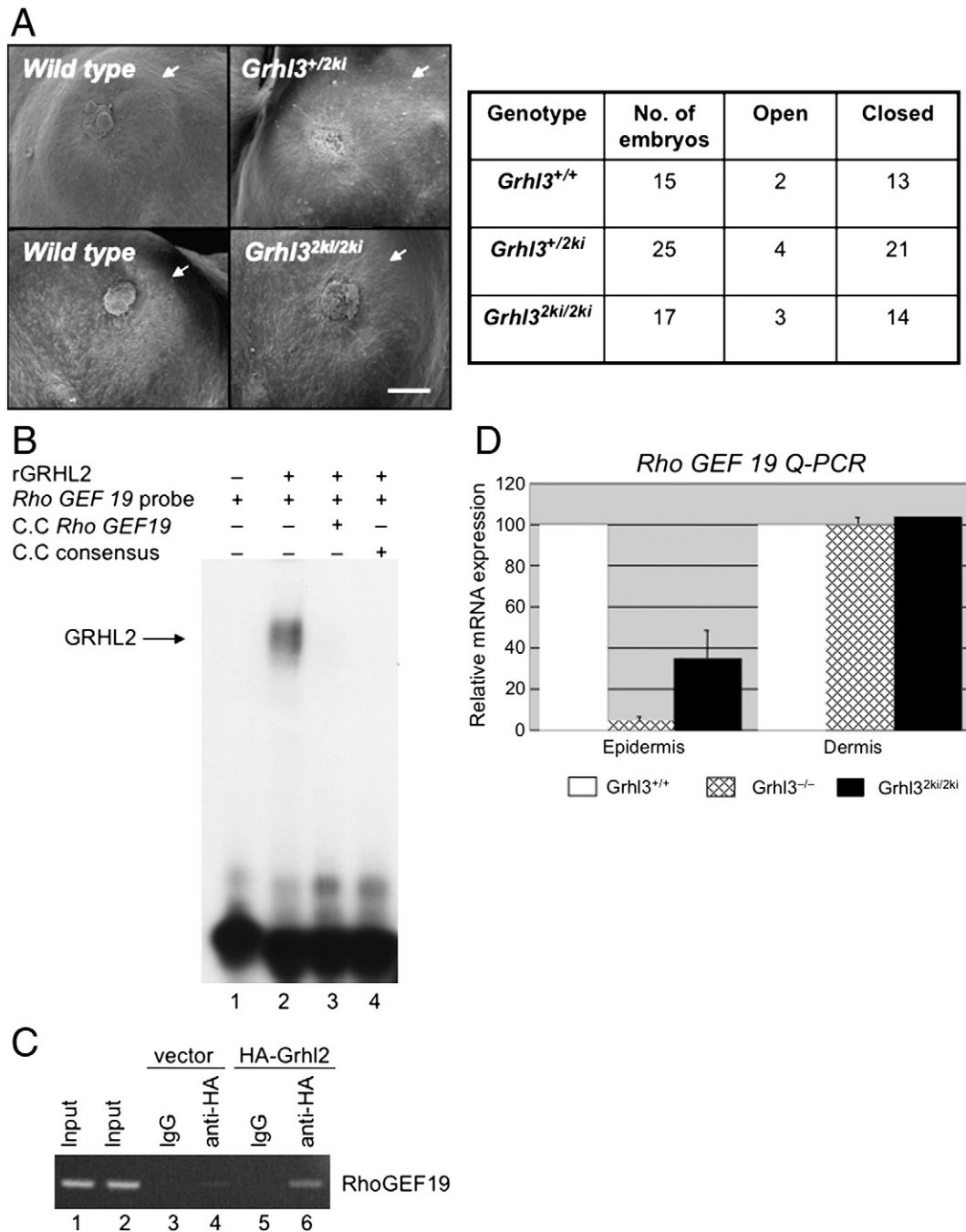
Fig. 6. *Grhl2* compensates for loss of *Grhl3* in embryonic wound repair through activation of *Rho GEF 19*. (A) SEM of hind limb amputation wounds after 24 h in culture in wild-type, *Grhl3−/2ki*, and *Grhl3²ki/2ki* embryos at E12.5. All images are representative of at least 15 embryos of each genotype. Arrows point to the boundary of the wound. Scale = 100 μm. The table is a summary of the wound healing data for the respective genotypes. A Fisher's exact test was used to determine statistical difference between wound healing for the different genotypes. *P* values ≤0.05 were considered significant. (B) EMSA of rGRHL2 with a *Rho GEF 19* probe. A 100-fold molar excess of unlabelled cold competitor *Grhl* consensus or *Rho GEF 19* probe was added in the indicated lanes. The migration of the GRHL2/DNA complexes is arrowed. (C) ChIP analysis of GRHL2 on the *Rho GEF 19* promoter. Chromatin from HaCAT cells transfected with empty vector (lane 4) or HA-tagged *Grhl2* (lane 6) was immunoprecipitated using antisera to the HA-tag. Pre-immune sera (lanes 3 and 5) served as negative controls. Lanes 1 and 2 show the input chromatin. The immunoprecipitated chromatin was amplified with *Rho GEF 19* primers. (D) Q-PCR of *Rho GEF 19* expression in wild-type (open columns), *Grhl3−/−* (hatched columns) and *Grhl3²ki/2ki* (closed columns) E18.5 epidermis and dermis. Bars represent standard errors. *HPRT* levels served as a reference.

gene dosage being the critical determinant of epidermal closure in these processes. Studies using compound heterozygous mice and the *Grhl3²ki* knock-in line demonstrate that three functional alleles of *Grhl2* or *Grhl3* are required for wound healing, with defective repair evident in *Grhl2+/−/Grhl3+/−* embryos, but not in the single heterozygotes, or in the *Grhl3²ki/2ki* mice. The EOB phenotype only manifests when functional alleles of *Grhl3* and *Grhl2* are reduced to one (*Grhl3−/−/Grhl2+/−* embryos), presumably reflecting the cooperative role of *Lmo4* in this process (Hislop et al., 2008). Our findings

in wound repair are similar to our analysis of the functional interaction between these two genes in another epidermal morphogenetic event regulated by this family, neural tube closure, where *Grhl2/Grhl3* compound heterozygotes exhibit incompletely penetrant exencephaly, which becomes fully penetrant with loss of one further *Grhl3* allele (Rifat et al., 2010). The similarities between these two apparently diverse epidermal morphogenetic events suggest that they may be regulated by a common *Grhl2/3*-dependent mechanism. Our studies in wound repair have identified *Rho GEF 19* as a critical GRHL3

target (Caddy et al., 2010), and we have confirmed here that this gene is also regulated by GRHL2. Taken together, these findings raise the possibility that *Rho GEF 19* plays a key role in neurulation as well as wound healing, a hypothesis that we are currently testing.

The overlapping roles of *Grhl3* and *Grhl2* in wound repair, eyelid fusion and neural tube closure coincide with the developmental co-expression of these genes, and is distinct from their disparate expression in late embryogenesis, when the skin barrier is forming (Auden et al., 2006). Although we have not formally excluded a role for *Grhl2* in establishing the barrier, the inability of the *Grhl3*^{2ki} alleles to compensate for loss of *Grhl3* in this process, coupled with the failure of GRHL2 to bind the *TGase1* promoter supports this conclusion. The generation of mice carrying a conditionally targetable allele of *Grhl2* will further address this issue. In contrast to *Grhl2*, *Grhl1* and *Grhl3* have more closely aligned epidermal expression patterns from E15.5 onwards, and yet display no functional redundancy in barrier formation. Loss of *Grhl1* manifests after birth with hair loss and PPK due to reduced expression of *Dsg1*. Expression of *Dsg1* is not altered in epidermis derived from *Grhl3*-null embryos (Yu et al., 2006), and consistent with this, we are unable to demonstrate binding of GRHL3 to the *Dsg1* regulatory elements. Similarly, GRHL1 does not localise to GRHL3 target sequences using ChIP. Thus, the unique and cooperative roles of the *Grhl* genes reflect their target gene specificity, which, given that the consensus sites of all three members is identical and the recombinant proteins display differential binding in isolation, must reflect the subtle differences we identified in their PWMs. Supporting this, the PWM of GRHL2 and GRHL3 are more closely aligned than GRHL1, providing a rationale for the greater functional overlap between the former two factors. A genome-wide ChIP-sequencing approach will shed further light on the in vivo target gene specificity of the three factors. Presumably, differences in their preferred protein partners may also influence downstream targets in some settings (Hislop et al., 2008).

The signalling pathways controlling eyelid closure display considerable overlap with those involved in epidermal wound healing and tumorigenesis (Xia and Kao, 2004). Mice with impaired activin signalling display EOB and delayed wound repair (Vassalli et al., 1994; Wankell et al., 2001), and c-Jun-null mice show reduced skin wound healing and tumor formation, similar to mice deficient in TGFα or EGFR signalling (Li et al., 2003; Zenz et al., 2003; Sibilia et al., 2000). In fact, *Grhl3* has been reported to function upstream of TGFα in the context of eyelid fusion (Yu et al., 2008). Interestingly, the epidermis in *Grhl3*-null (and *Grhl3*$^{2ki/2ki}$) embryos exhibits marked hyperproliferative changes and altered keratinocyte differentiation (Ting et al., 2005; Yu et al., 2006), features associated with skin tumor formation (Ridky and Khavari, 2004). Determining whether mice with a deletion of *Grhl3* or *Grhl2* in the adult epidermis exhibit susceptibility to skin cancers will be of interest. Another signalling cascade implicated in EOB and wound repair is the planar cell polarity (PCP) pathway. Mice carrying mutations in the *Vangl2* (Kibar et al., 2001), *Scrb1* (Murdoch et al., 2003), *Celsr1* (Curtin et al., 2003), *PTK7* (Lu et al., 2004) and *Grhl3* (Hislop et al., 2008) genes, all components of the PCP pathway, exhibit EOB. These mutant strains also display defective wound repair, either in the homozygous state (*PTK7*, *Celsr1*, *Scrb1*, *Grhl3*), or as compound heterozygotes (*Vangl2/Scrb1*, *Vangl2/Grhl3*) (Caddy et al., 2010). Neural tube defects are also a feature of PCP mutant strains, and on this basis, it seems certain that *Grhl2* will also play a role in PCP signalling in the context of all three epidermal morphogenetic events.

Acknowledgments

Appendix A. Supplementary data

Supplementary data to this article can be found online at doi:10.1016/j.ydbio.2010.11.011.

References

Attardi, L.D., Von Seggern, D., Tjian, R., 1993. Ectopic expression of wild-type or a dominant-negative mutant of transcription factor NTF-1 disrupts normal Drosophila development. Proc. Natl Acad. Sci. USA 90, 10563–10567.
Auden, A., Caddy, J., Wilanowski, T., Ting, S.B., Cunningham, J.M., Jane, S.M., 2006. Spatial and temporal expression of the Grainyhead-like transcription factor family during murine development. Gene Expr. Patterns 6, 964–970.
Biggin, M.D., Tjian, R., 1988. Transcription factors that activate the Ultrabithorax promoter in developmentally staged extracts. Cell 53 699-11.
Bray, S.J., Kafatos, F.C., 1991. Developmental function of Elf-1: an essential transcription factor during embryogenesis in Drosophila. Genes Dev. 5, 1672–1683.
Caddy, J., Wilanowski, T., Darido, C., Dworkin, S., Ting, S.B., Zhao, Q., Rank, G., Auden, A., Srivastava, S., Papenfuss, T.A., Murdoch, J.N., Humbert, P.O., Parekh, V., Boulos, N., Weber, T., Zuo, J., Cunningham, J.M., Jane, S.M., 2010. Epidermal wound repair is regulated by the planar cell polarity signaling pathway. Dev. Cell 19, 138–147.
Colas, J.F., Schoenwolf, G.C., 2001. Towards a cellular and molecular understanding of neurulation. Dev. Dyn. 221, 117–145.
Curtin, J.A., Quint, E., Tsipouri, V., Arkell, R.M., Cattanach, B., Copp, A.J., Henderson, D.J., Spurr, N., Stanier, P., Fisher, E.M., Nolan, P.M., Steel, K.P., Brown, S.D., Gray, I.C., Murdoch, J.N., 2003. Mutation of Celsr1 disrupts planar polarity of inner ear hair cells and causes severe neural tube defects in the mouse. Curr. Biol. 13, 1129–1133.
Dynlacht, B.D., Attardi, L.D., Admon, A., Freeman, M., Tjian, R., 1989. Functional analysis of NTF-1, a developmentally regulated Drosophila transcription factor that binds neuronal cis elements. Genes Dev. 3, 1677–1688.
Findlater, G.S., McDougall, R.D., Kaufman, M.H., 1993. Eyelid development, fusion and subsequent reopening in the mouse. J. Anat. 183, 121–129.
Forsberg, E.C., Downs, K.M., Christensen, H.M., Im, H., Nuzzi, P.A., Bresnick, E.H., 2000. Developmentally dynamic histone acetylation pattern of a tissue-specific chromatin domain. Proc. Natl Acad. Sci. USA 97, 14494–14499.
Grose, R., 2003. Epithelial migration: open your eyes to c-Jun. Curr. Biol. 13, R678–R680.
Hackett, D.A., Smith, J.L., Schoenwolf, G.C., 1997. Epidermal ectoderm is required for full elevation and for convergence during bending of the avian neural plate. Dev. Dyn. 210, 397–406.
Hardman, M.J., Sisi, P., Banbury, D.N., Byrne, C., 1998. Patterned acquisition of skin barrier function during development. Development 125, 1541–1552.
Hislop, N.R., Caddy, J., Ting, S.B., Auden, A., Vasudevan, S., King, S.L., Lindeman, G.J., Visvader, J.E., Cunningham, J.M., Jane, S.M., 2008. Grhl3 and Lmo4 play coordinate roles in epidermal migration. Dev. Biol. 321, 263–272.
Jacinto, A., Martin, P., 2001. Morphogenesis: unravelling the cell biology of hole closure. Curr. Biol. 11, R705–R707.
Jacinto, A., Martinez-Arias, A., Martin, P., 2001. Mechanisms of epithelial fusion and repair. Nat. Cell Biol. 3, E117–E123.
Jane, S.M., Ting, S.B., Cunningham, J.M., 2005. Epidermal impermeable barriers in mouse and fly. Curr. Opin. Genet. Dev. 15, 447–453.
Kibar, Z., Vogan, K.J., Groulx, N., Justice, M.J., Underhill, D.A., Gros, P., 2001. Ltap, a mammalian homolog of Drosophila Strabismus/Van Gogh, is altered in the mouse neural tube mutant Loop-tail. Nat. Genet. 28, 251–255.
Kudryavtseva, E.I., Sugihara, T.M., Wang, N., Lasso, R.J., Gudnason, J.F., Lipkin, S.M., Andersen, B., 2003. Identification and characterization of Grainyhead-like epithelial transactivator (GET-1), a novel mammalian Grainyhead-like factor. Dev. Dyn. 226, 604–617.
Lee, H., Adler, P.N., 2004. The grainy head transcription factor is essential for the function of the frizzled pathway in the Drosophila wing. Mech. Dev. 121, 37–49.
Li, G., Gustafson-Brown, C., Hanks, S.K., Nason, K., Arbeit, J.M., Pogliano, K., Wisdom, R.M., Johnson, R.S., 2003. c-Jun is essential for organization of the epidermal leading edge. Dev. Cell 4, 865–877.
Lu, X., Borchers, A.G., Jolicoeur, C., Rayburn, H., Baker, J.C., Tessier-Lavigne, M., 2004. PTK7/CCK-4 is a novel regulator of planar cell polarity in vertebrates. Nature 430, 93–98.
Mace, K.A., Pearson, J.C., McGinnis, W., 2005. An epidermal barrier wound repair pathway in Drosophila is mediated by grainy head. Science 308, 381–385.
Madison, K.C., 2003. Barrier function of the skin: "la raison d'etre" of the epidermis. J. Invest. Dermatol. 121, 231–241.
Martin, P., 1996. Mechanisms of wound healing in the embryo and fetus. Curr. Top. Dev. Biol. 32, 175–203.
Murdoch, J.N., Henderson, D.J., Doudney, K., Gaston-Massuet, C., Phillips, H.M., Paternotte, C., Arkell, R., Stanier, P., Copp, A.J., 2003. Disruption of scribble (Scrb1) causes severe neural tube defects in the circletail mouse. Hum. Mol. Genet. 12, 87–98.
Narasimha, M., Uv, A., Krejci, A., Brown, N.H., Bray, S.J., 2008. Grainy head promotes expression of septate junction proteins and influences epithelial morphogenesis. J. Cell Sci. 121, 747–752.
Ostrowski, S., Dierick, H.A., Bejsovec, A., 2002. Genetic control of cuticle formation during embryonic development of Drosophila melanogaster. Genetics 161, 171–182.
Proksch, E., Brandner, J.M., Jensen, J.M., 2008. The skin: an indispensable barrier. Exp. Dermatol. 17, 1063–1072.

Ridky, T.W., Khavari, P.A., 2004. Pathways sufficient to induce epidermal carcinogenesis. Cell Cycle 3, 621–624.

Rifat, Y., Parekh, V., Wilanowski, T., Hislop, N.R., Auden, A., Ting, S.B., Cunningham, J.M., Jane, S.M., 2010. Regional neural tube closure defined by the Grainy head-like transcription factors. Dev. Biol. 345, 237–245.

Segre, J., 2003. Complex redundancy to build a simple epidermal permeability barrier. Curr. Opin. Cell Biol. 15, 776–782.

Segre, J.A., 2006. Epidermal barrier formation and recovery in skin disorders. J. Clin. Invest. 116, 1150–1158.

Sibilia, M., Fleischmann, A., Behrens, A., Stingl, L., Carroll, J., Watt, F.M., Schlessinger, J., Wagner, E.F., 2000. The EGF receptor provides an essential survival signal for SOS-dependent skin tumor development. Cell 102, 211–220.

Ting, S.B., Wilanowski, T., Auden, A., Hall, M., Voss, A.K., Thomas, T., Parekh, V., Cunningham, J.M., Jane, S.M., 2003a. Inositol- and folate-resistant neural tube defects in mice lacking the epithelial-specific factor Grhl-3. Nat. Med. 9, 1513–1519.

Ting, S.B., Wilanowski, T., Cerruti, L., Zhao, L.L., Cunningham, J.M., Jane, S.M., 2003b. The identification and characterization of human Sister-of-Mammalian Grainyhead (SOM) expands the grainyhead-like family of developmental transcription factors. Biochem. J. 370, 953–962.

Ting, S.B., Caddy, J., Hislop, N., Wilanowski, T., Auden, A., Zhao, L.L., Ellis, S., Kaur, P., Uchida, Y., Holleran, W.M., Elias, P.W., Cunningham, J.M., Jane, S.M., 2005. A homolog of Drosophila grainy head is essential for epidermal integrity in mice. Science 308, 411–413.

Uv, A.E., Harrison, E.J., Bray, S.J., 1997. Tissue-specific splicing and functions of the Drosophila transcription factor Grainyhead. Mol. Cell. Biol. 17, 6727–6735.

Vassalli, A., Matzuk, M.M., Gardner, H.A., Lee, K.F., Jaenisch, R., 1994. Activin/inhibin beta B subunit gene disruption leads to defects in eyelid development and female reproduction. Genes Dev. 8, 414–427.

Venkatesan, K., McManus, H.R., Mello, C.C., Smith, T.F., Hansen, U., 2003. Functional conservation between members of an ancient duplicated transcription factor family, LSF/Grainyhead. Nucleic Acids Res. 31, 4304–4316.

Vlieghe, D., Sandelin, A., De Bleser, P.J., Vleminckx, K., Wasserman, W.W., van Roy, F., Lenhard, B., 2006. A new generation of JASPAR, the open access repository for transcription factor binding site profiles. Nucleic Acids Res. 34, D95–D97.

Wankell, M., Munz, B., Hubner, G., Hans, W., Wolf, E., Goppelt, A., Werner, S., 2001. Impaired wound healing in transgenic mice overexpressing the activin antagonist follistatin in the epidermis. EMBO J. 20, 5361–5372.

Wilanowski, T., Tuckfield, A., Cerruti, L., O'Connell, S., Saint, R., Parekh, V., Tao, J., Cunningham, J.M., Jane, S.M., 2002. A highly conserved novel family of mammalian developmental transcription factors related to Drosophila grainyhead. Mech. Dev. 114, 37–50.

Wilanowski, T., Caddy, J., Ting, S.B., Hislop, N.R., Cerruti, L., Auden, A., Zhao, L.L., Asquith, S., Ellis, S., Sinclair, R., Cunningham, J.M., Jane, S.M., 2008. Perturbed desmosomal cadherin expression in grainy head-like 1-null mice. EMBO J. 27, 886–897.

Xia, Y., Kao, W.W., 2004. The signaling pathways in tissue morphogenesis: a lesson from mice with eye-open at birth phenotype. Biochem. Pharmacol. 68, 997–1001.

Xia, Y., Karin, M., 2004. The control of cell motility and epithelial morphogenesis by Jun kinases. Trends Cell Biol. 14, 94–101.

Yu, Z., Lin, K.K., Bhandari, A., Spencer, J.A., Xu, X., Wang, N., Lu, Z., Gill, G.N., Roop, D.R., Wertz, P., Andersen, B., 2006. The Grainyhead-like epithelial transactivator Get-1/Grhl3 regulates epidermal terminal differentiation and interacts functionally with LMO4. Dev. Biol. 299, 122–136.

Yu, Z., Bhandari, A., Mannik, J., Pham, T., Xu, X., Andersen, B., 2008. Grainyhead-like factor Get1/Grhl3 regulates formation of the epidermal leading edge during eyelid closure. Dev. Biol. 319, 56–67.

Zenz, R., Scheuch, H., Martin, P., Frank, C., Eferl, R., Kenner, L., Sibilia, M., Wagner, E.F., 2003. c-Jun regulates eyelid closure and skin tumor development through EGFR signaling. Dev. Cell 4, 879–889.

Zhang, L., Wang, W., Hayashi, Y., Jester, J.V., Birk, D.E., Gao, M., Liu, C.Y., Kao, W.W., Karin, M., Xia, Y., 2003. A role for MEK kinase 1 in TGF-beta/activin-induced epithelium movement and embryonic eyelid closure. EMBO J. 22, 4443–4454.